

# Network Pharmacology and Experimental Verification Reveal a Protective Role of Jiedu Tongluo Tiaogan Formula on INS-1 Cells and HepG2 Cells From High Glucose-mediated Injury via the PI3K/Akt Pathways

**Qi Zhang**

Changchun University of Chinese Medicine

**Chunli Piao** (✉ [pcl2013@sina.cn](mailto:pcl2013@sina.cn))

Guangzhou University of Chinese Medicine

**Wenqi Jin**

Changchun University of Chinese Medicine

**De Jin**

China Academy of Chinese Medical Sciences Guanganmen Hospital

**Han Wang**

China Academy of Chinese Medical Sciences Guanganmen Hospital

**Cheng Tang**

Changchun University of Chinese Medicine

**Xiaohua Zhao**

Shenzhen Futian Hospital

**Naiwen Zhang**

Shenzhen Futian Hospital

**Shengnan Gao**

Shenzhen Futian Hospital

**Fengmei Lian**

China Academy of Chinese Medical Sciences Guanganmen Hospital

---

## Research

**Keywords:** Jiedu Tongluo Tiaogan Formula, Type 2 diabetes mellitus, network pharmacology, PI3K/AKT signaling pathway, Traditional Chinese medicine

**Posted Date:** June 30th, 2021

**DOI:** <https://doi.org/10.21203/rs.3.rs-658131/v1>

**License:** © ⓘ This work is licensed under a Creative Commons Attribution 4.0 International License.

[Read Full License](#)

---

**Network pharmacology and experimental verification reveal an protective role of Jiedu Tongluo Tiaogan Formula on INS-1 cells and HepG2 cells from high glucose-mediated injury via the PI3K/Akt Pathways**

**Authors:**

Qi Zhang<sup>1#</sup>, Chunli Piao<sup>2##</sup>, Wenqi Jin<sup>3</sup>, De Jin<sup>4</sup>, Han Wang<sup>4</sup>, Cheng Tang<sup>1</sup>, Xiaohua Zhao<sup>2</sup>, Naiwen Zhang<sup>2</sup>, Shengnan Gao<sup>2</sup>, Fengmei Lian<sup>4</sup>

**1** Changchun University of Chinese Medicine, Changchun 130000, Jilin, China

**2** Shenzhen Hospital, Guangzhou University of Chinese Medicine (Futian), Shenzhen 518000, Guangdong, China

**3** Research Center of Traditional Chinese Medicine, The Affiliated Hospital to Changchun University of Chinese Medicine, Changchun 130021, Jilin, China

**4** Guang'anmen Hospital, China Academy of Chinese Medical Science, Beijing 100000, China

**# The co-first authors:**

Qi Zhang(e-mail:596058757@qq.com), Chunli Piao(e-mail:pcl2013@sina.cn),

**\*Correspondence:**

Chunli Piao

Shenzhen Hospital, Guangzhou University of Chinese Medicine (Futian), 6001 North Ring Road, Futian District, Shenzhen 518000, Guangdong, China. Tel.: +86-18819075590. Email:pcl2013@sina.cn.

## **Abstract**

**Background:** T2DM is considered to be a chronic low-grade inflammatory disease, because of its high morbidity and mortality, diabetes poses a tremendous potential threat to public health. Our previous studies have shown that a traditional Chinese medicine formula, Jiedu Tongluo Tiaogan Formula (JDTL) exerts favorable hypoglycemic effect, however, its molecular mechanism and the interaction among various components need to be further elucidated. This study aimed to explore the mechanism of JDTL in the treatment of T2DM using an integrated strategy of system pharmacology, bioinformatics analysis, and experimental verification.

**Materials and Methods:** First, the compounds of JDTL were searched from public databases, and the "compound-target" network was constructed to predict the potential active components and targets. Subsequently, bioinformatics analysis was used to identify potential targets and signaling pathways, including PPI, GO pathways and KEGG pathways. Finally, the pharmacological effects and mechanisms of JDTL were verified by molecular docking and cell experiments.

**Results:** Analysis by GO and KEGG pathway enrichment revealed that these targets were associated with lipopolysaccharide, membrane microdomain, cytokine receptor binding, and JDTL could regulate the PI3K/Akt signaling pathway. Furthermore, we have proved that JDTL could improve the mRNA expression and protein expression of IRS1, AKT, and PI3K in the INS-1 cell and HepG2 cells.

**Conclusion:** The present study elucidated the active ingredients, potential targets, and molecular mechanism of JDTL in the treatment of T2DM, and revealed the characteristics of JDTL in multi-component, multi-target and multi-channel. It also provided an important scientific basis for new drug development and mechanism research of T2DM.

**Keywords:** Jiedu Tongluo Tiaogan Formula, Type 2 diabetes mellitus, network pharmacology, PI3K/AKT signaling pathway, Traditional Chinese medicine

## **Introduction**

Type 2 diabetes mellitus (T2DM) is considered to be a chronic low-grade inflammatory disease characterized by insulin resistance and pancreatic  $\beta$  cell dysfunction<sup>1</sup>. Generally, if diabetes is not well controlled, it can cause serious complications, including heart attacks, kidney failure, optic nerve damage, and nerve damage<sup>2,3</sup>. In addition, because of its high incidence rate and high mortality rate, diabetes poses a huge potential threat to public health<sup>4</sup>. However, the current research on the pathogenesis of T2DM has not yet fully clarified, and its pathogenesis may be related to factors such as family history, obesity, poor diet and lack of exercise<sup>5</sup>. Although hypoglycemic drugs and insulin are mainly used in the treatment of patients with T2DM, there are still great challenges to improve the condition of patients. Clinical practice supported by randomized clinical trials shows that in a large proportion of patients with T2DM, diabetes medication alone cannot achieve blood glucose goals<sup>6</sup>. Therefore, there is an urgent need for more alternative treatment for patients with clinical treatment.

Traditional Chinese medicine (TCM) treats diseases based on a holistic view, which believes that all body systems are interconnected. Therefore, TCM has the advantages of pleiotropic, multi-target, prospective, and stable in the treatment of T2DM and other chronic diseases<sup>7</sup>. TCM has the effects of synergistically lowering blood sugar, improving symptoms, improving mood, improving metabolism, improving quality of life, and protecting target organs. Therefore, as an important supplement and alternative medicine, it can bring beneficial effects to patients with T2DM, and it has been widely accepted worldwide<sup>8</sup>. One such agent, Jiedu Tongluo Tiaogan Formula (JDTL), was formulated based on TCM theory. It consists of five herbal medicines, namely, *Coptis chinensis* Franch (Huanglian), *Radix Rhei Et Rhizome* (Dahuang), *Astragalus propinquus* Schischkin (Huangqi), *Salvia miltiorrhiza* Bunge (Danshen) and *Bupleuri Radix* (Chaihu), with a compatible dosage of 15:9:15:15:10. A clinical study showed that the combined application of JDTL might be effective and tolerated in reducing blood glucose, glycosylated hemoglobin and insulin secretion in obese patients with T2DM<sup>9</sup>. A basic study suggested that JDTL

can improve insulin resistance and reduce apoptosis of cells, and further increase glucose and lipid metabolism in type 2 diabetic rats<sup>10</sup>. Other studies showed that JDTL may inhibit inflammation-related factors, promote the secretion of adiponectin, reduce the inflammatory response of adipocytes, and relieve endoplasmic reticulum stress in a multi-target manner<sup>11</sup>. Therefore, more and more evidence shows that JDTL exerts favorable hypoglycemic effect. However, little is accepted about the pharmacodynamic actual base and atomic biological apparatus of JDTL in the treatment of T2DM.

Network pharmacology provides a new research paradigm for the transformation of TCM from empirical medicine to evidence-based medicine, and has become an indispensable method to explore the potential mechanism of TCM<sup>12</sup>. Network pharmacology is based on systems biology, combined with multi-directional pharmacology, by constructing multiple networks to explain the relationship between drugs, molecules, targets, diseases and pathways, and explains the molecular mechanism of TCM prescription from a more comprehensive perspective, which is also consistent with the holistic view of TCM in the treatment of diseases<sup>13</sup>. For example, network pharmacology method is used to define the active ingredients and potential targets in Milkwitch root for the treatment of diabetic nephropathy<sup>14</sup>.

The study was aimed at investigating the potential targets of JDTL in the treatment of T2DM and to explore its mechanism. First, the active ingredients and potential mechanism of JDTL were analyzed by network pharmacology. Then, the molecular docking was used to verify the binding strength between the compound in JDTL and the hub gene. Finally, through a series of in vitro experiments, the mechanism of JDTL in the main signaling pathway of INS-1 cell and HepG2 cells network pharmacological integration was explored in order to further study the mechanism of JDTL in the treatment of T2DM. The workflow of this study was shown in Figure 1.

## **Materials and Methods**

### Screening the Active Components

Oral bioavailability (OB) and drug similarity (DL) are two important parameters

to evaluate the active components of drugs in drug research and development, which respectively reflect the absorption and distribution of drugs in human body. These ingredients can be similar to existing drugs. And pre-proving the possibility of developing drugs. In this present study, the active compounds of JDTL were screened with  $OB \geq 30\%$  and  $DL \geq 0.18$ . Next, the targets were transformed using the UniProt knowledge database (<https://www.uniprot.org/>).

#### Identification of Gene Targets for T2DM

Data on the T2DM targets were obtained from two databases. At first, the GeneCards v4.14 (<http://www.genecards.org/>) network library is searched for its related targets, and a correlation value of  $\geq 30$  was used as the screening parameters. The other source was Online Mendelian Inheritance in Man (OMIM) (<http://www.omim.org/>). At last, in adjustment to ensure the accurateness of the ambition database, redundant and erroneous targets need to be removed.

#### Network Construction

TCM is a multi-component, multi-target system. To better clarify the complex relationship between compounds, targets and disease pathways, the network visualization analysis software Cytoscape (<http://www.cytoscape.org/>) was used to draw the compound-target (C-T) network and target-pathway (T-P) network. Meanwhile, we intersect drug targets with genes related to T2DM and illustrate the intersection with Venn diagram.

#### Construction of a Protein-Protein Interaction (PPI) Network

The common targets related to drug targets with the genes that were associated with T2DM were imported into the STRING database (<https://string-db.org/>) to maintain their interaction relationship with the species limited to "Homo sapiens" and a confidence score  $> 0.9$ . In addition, the results were analyzed in Cytoscape 3.7.2 to set up a PPI network.

#### Enrichment of Gene Ontology (GO) Pathway and the Kyoto Encyclopedia of Genes and Genomes (KEGG) Pathway

In order to investigate the cell functions and signaling pathways that were mainly

affected by the key targets for JDTL treatment of T2DM, We use clusterProfile version3.6.2 of the R package in Bioconductor (<http://www.bioconductor.org/about/>) to perform GO function enrichment analysis on common targets, draw GO analysis entry diagrams, and understand their biological processes (BP) and molecular functions (MF) and cell component (CC), the screening condition is  $P < 0.05$ . And the common target was enriched by KEGG pathway ( $P < 0.05$ ), the results were shown in bubble chart.

#### Molecular Docking

SYBYL software is simulation software for the molecule docking analysis of small molecules and biological macromolecules. Through high-precision docking simulation and molecular dynamics analysis, the mechanism of ligands acting on complex molecular networks is clarified. We used Sybyl software to evaluate the potential of integration between the selected target and JDTL.

#### Preparation of the JDTL formula

The herbs of JDTL were provided by the Department of Pharmacy, the Affiliated Hospital of Changchun University of Chinese Medicine (Jilin, China). Briefly, 15g Huanglian (*Coptis chinensis* Franch), 9g Dahuang (*Radix Rhei Et Rhizome*), 15g Huangqi (*Astragalus propinquus* Schischkin), 15g Danshen (*Salvia miltiorrhiza* Bunge), and 10g Chaihu (*Bupleuri Radix*) in 1000 mL reverse osmosis water were simmered to 250mL to obtain an extract. Then, JDTL formula was prepared by freeze-drying technology. The powder was dissolved in 100 mg/mL concentrated solution with deionized water, filtered (0.2  $\mu\text{m}$ ), sterilized, and diluted for biological studies. In order to ensure the quality of JDTL, we analysed the composition of JDTL by high-performance liquid chromatography (HPLC). Five major peaks of JDTL extract were identified using HPLC (Figure 2). As shown in Figure 2, Chlorogenic acid, Calycosin-7-glucoside, Salvianolic acid B, Aloe-emodin, and Haragoside in JDTL were identified by comparing the retention time from high-performance liquid chromatography with good reproducibility.

#### Cells and Cell Culture

INS-1 cells and HepG2 cells were purchased from the Cell Center of Peking

Union Medical College Hospital and individually cultured in RPMI-1640 medium (Gibco, US), DMEM (Gibco; Thermo Fisher Scientific, Inc.) containing 10% fetal bovine serum, 100 U/mL penicillin and 100 µg/mL streptomycin at 37 °C, 5% CO<sub>2</sub> and relatively saturated humidity. Throughout the entire cell culture process, the principle of sterility was strictly observed. In order to explore the effect and mechanism of JDTL, INS-1 cells and HepG2 cells were incubated with 30 mM glucose for 24 hours, in the presence or absence of JDTL (50-200 mg/mL). Meanwhile, the cells in control group were cultured in DMEM or 1640 medium for 24 h. The cells were used for subsequent experimentation upon attaining a logarithmic growth phase.

#### Cell viability

INS-1 cells and HepG2 cells were respectively seeded onto 96-well plates (10<sup>4</sup> cells/well) for 24 hours prior to supplementation with JDTL of known concentration (0, 50, 100, 200, 500 mmol/L). Next, spent medium was removed and replaced with MTT (3-(4,5-dimethylthiazol-2-yl)-2, 5-diphenyltetrazolium bromide) solution (0.5mg/mL in PBS) to incubation of cells for 4 h at 37 °C. Then, 150 µL DMSO was added to each well then absorbance readings (at 570 nm) were recorded using a microplate reader (TECANA-5082, Magellan, Austria).

#### Glucose-stimulated insulin secretion (GSIS)

The INS-1 cells (1×10<sup>5</sup> cells/well) were seeded in 96-well plates with glucose (5 or 30 mM) for 48 h and then incubated with 0, 50, 100, 200 µg/mL JTTF for 24 h. After that, the cells were washed with PBS thoroughly and incubated with Krebs-Ringer bicarbonate HEPES buffer (KRBB, 4.8 mM KCl, 129 mM NaCl, 2.5 mM CaCl<sub>2</sub>, 1.2 mM KH<sub>2</sub>PO<sub>4</sub>, 1.2 mM MgSO<sub>4</sub>, 20 mM HEPES, 5 mM NaHCO<sub>3</sub>, and 0.5% bovine serum albumin (BSA), pH 7.4) for 1 h. The buffer was replaced by KRB buffer with 5 mmol/L glucose (low glucose) or 30 mmol/L glucose (high glucose), and incubated at 37°C for 1 h. The supernatant was collected respectively. The insulin in the supernatant was determined using a Rat/Mouse Insulin Elisa Kit (Millipore, USA).

### Glucose uptake assay

HepG2 cells were seeded into 24-well cell culture plates. Following 24 h of stabilization, the cells were incubated with different drugs for 24 h. Then, the medium was removed and the cells were washed once with PBS, followed by incubation with 100 nM insulin for 30 min. After incubation, cells were exposed to 50  $\mu$ M 2-NBDG for another 30 min. Then, the supernatant was discarded and washed twice with ice-cold PBS, and 2-NBDG fluorescence intensity was measured with a fluorescence microplate reader (Varioskan LUX, Thermo Fisher, USA) at an excitation wavelength of 485 nm and emission wavelength of 538 nm.

### Total RNA preparation and real-time PCR

Total RNA was extracted from INS-1 cells and HepG2 cells using the TRIzol reagent (TIANGEN, Beijing, China) and reverse transcribed using the First Strand cDNA synthesis kit (TaKaRa, Dalian, China) according to manufacturer's instructions. The RT-qPCR procedure was performed as follows: predenaturation at 95°C for 15 min and 40 cycles of denaturation at 95 °C for 10s, annealing at 60°C for 20s, and elongation at 72 °C for 30s. The primers used to amplify PI3K, Akt, and GAPDH genes, were synthesized by Invitrogen (Thermo Fisher Scientific, Inc.):

PI3K Forward GCTGTTGATAGACCACCGCTTCC

Reverse TGCCCTGTTCCTCTGCCTTCC

Akt Forward CAGGAGGAGGAGACGATGGACTTC

Reverse CACACGGTGCTTGGGCTTGG

GAPDH Forward TGGTGGACCTCATGGCCTAC

Reverse CAGCAACTGAGGGCCTCTCT

The expression level of GAPDH was used as internal control.

### Western blot analysis

Western blot procedures were performed as previously described<sup>15</sup>. Then, INS-1 cells and HepG2 cells that received different treatments were harvest and lysed with RIPA lysis buffer (Beyotime Biotechnology, Jiangsu, China) supplemented with protease and phosphatase inhibitors (Roche, Mannheim, Germany). The following

primary antibodies were used: The anti-IRS, anti-phosphor- Ser612- IRS-1, anti-PI3K, anti-phosphor-Thy458-PI3K, anti-Akt, anti-phosphor-Ser473-Akt, and anti- $\beta$ -action were from Cell Signaling Technology (Danvers, MA). Quantification of the relative change in protein levels (arbitrary unit; expressed as percentage of the control protein level) was performed by using image J program.

#### Statistical Analysis

GraphPad Prism 6.0 software was used for statistical analysis of the data. Data are presented as mean  $\pm$  SD from three different experiments. The results were considered statistically significant at  $P < 0.05$ .

## Results

### Targets Fishing

A total of 205 active compounds were selected by searching in the specified database (Table 1). Afterwards, a total of 871 T2DM-related target genes were selected in OMIM and GeneCards databases. Then, we entered drug targets and disease targets in Venny 2.1. After eliminating redundancy, we found that JDTL and T2DM 110 share common targets as shown in Figure 3.

### Analyses of a PPI Network

The common targets were imported into the STRING database, and then the visualization of the relationship between these common goals was obtained. The average node degree in this PPI network is 15.4 and the PPI network consisting of 110 nodes and 849 edges (Figure 4(a)). In order to better explain the relationship between targets, TSV data were imported into Cytoscape, and in this network, node sizes and colors reflect the number of combined targets (degree) (Figure 4(b)).

The degree values of the first 30 genes are shown in Figure 4(c), which includes RAC-alpha serine/threonine-protein kinase (AKT1), interleukin-6 (IL-6), vascular endothelial growth factor A (VEGFA), mitogen-activated protein kinase 1(MAPK1), mitogen-activated protein kinase8(MAPK8), Transcription factor AP-1(JUN), Pro-epidermal growth factor (EGF), Epidermal growth factor receptor (EGFR), Interleukin-8(CXCL8), and Interleukin-1 beta (IL1B) etc. In Figure 4(c), In Figure 4(c), the x-axis represents the number of adjacent proteins of the target protein. The

y-axis represents the target protein.

As shown in Figure 4(c), AKT1 may be related to 58 other proteins, IL6 may be related to 51 other proteins, VEGFA may be related to 49 other proteins, MAPK1 and MAPK8 may be related to the 47 other proteins, JUN, EGF, EGFR, CXCL8 and IL1B may be related to the 45, 40, 39, 38, and 37 other proteins, respectively. At the same time, we used the top 10 proteins to dock with the active compounds in JDTL to verify their interaction ability.

### **Analyses of Enrichment of the GO Pathways and KEGG Pathways**

Taking into account the complex mechanism of JDTL treatment of T2DM, and then by integrating the key paths in the GO database and the KEGG database, a complete T2DM related path diagram was constructed. GO Pathways and KEGG Pathways analysis were performed using R software. Go analysis is used to characterize molecular function (MF), cellular composition (CC) and biological process (BP) of genes. As shown in Figure 5(a,b,c), the T2DM-related pathways were involved in several biological functions, such as lipopolysaccharide, oxidative stress, cell proliferation, membrane microdomain, cytokine receptor binding, and cytokine activity. As for pathway analysis, the 73 targets participate in top 20 KEGG pathways with significant P-value < 0.05 including PI3K-Akt signaling pathway and so on (Figure 6). Furthermore, results of the first 20 KEGG pathways analyses are apparent in Table 2. The mechanism of JDTL in the treatment of T2DM may be realized by regulating these biological functions.

### **Network Analysis**

A compound-compound target (C-T) network constructed by active ingredients and their targets of JDTL formula was constructed by Cytoscape 3.7.2 software. Meanwhile, a target-pathway (C-P) network constructed by the top 20 KEGG pathways and their targets was also constructed by Cytoscape 3.7.2 software (Figures 7 and 8). In addition, In the C-T network, the median values of “degree”, “betweenness” and “closeness” were 1,0, 0.39, and in the C-P network, the median values of “degree” “betweenness” and “closeness” were 1,0, 0.667, respectively.

### **Docking Results Analysis**

In this study, molecular docking was used to identify the binding ability between the bioactive components of JDTL and hub gene<sup>16</sup>. In this docking assay, ten human receptors were retrieved from PDB: AKT1 (PDB ID: 1UNQ: 0.98Å), IL-6(PDB ID: 4CNI: 2.20Å), VEGFA (PDB ID: 3V2A: 3.20Å), MAPK1(PDB ID:4iz5:3.19 Å), MAPK8(PDB ID: 4YR8: 2.40 Å), JUN (PDB ID: 1S9K: 3.10 Å), EGF (PDB ID: 2KV4), EGFR (PDB ID: 5WB7: 2.94 Å), CXCL8(PDB ID: 2IL8), IL1B (PDB ID: 4DEP: 3.10 Å). 10 hub genes were entered into SYBYL 21 to check the molecular docking. The docking scores were greater than 5 indicating that they had good binding activity. In Figure 9, the results indicated that the bioactive components of JDTL demonstrated good binding with the hub genes. Furthermore, the after-effects of the molecular docking are apparent in Table 3.

#### **Effect of JDTL on cell viability**

The result of MTT assay demonstrated that JDTL at 50, 100, and 200 µg/mL had no effect on the viability of INS-1 cells and HepG2 cells, after treatment for 24 h (Figure 10), which were chosen in subsequent experiments.

#### **GSIS And Glucose Uptake Analysis**

The results of GSIS showed that after 5.0 mM low glucose starvation for 1 h, the INS-1 cells were stimulated by glucose at a normal level in the 5.0 mM group, and the insulin secretion of INS-1 cells decreased in the HG groups. Following the same glucose starvation, the INS-1 cells were stimulated by glucose at a high glucose level in the 30 mM group, the insulin secretion level of INS-1 cells decreased compared to the control group. As a result, the insulin secretion function was greatly improved by JDTL treatment (Figure 11). In addition, HepG2 cells were exposed to 30 mM glucose for 24 h followed by insulin (100 nM) incubation for 30 min. Compared to the normal control cells, an obvious decrease of 2-NBDG uptake was exhibited in model cells. The uptake of HepG2 cells was enhanced in each JDTL treatment group (Figure 12).

#### **Effect of JDTL on the PI3K/Akt signaling pathway**

The mRNA expression of PI3K and Akt in INS-1 cells and HepG2 cells

The mRNA expression levels of PI3K and Akt were detected by qRT-PCR. As

shown in Figure 13(a,b) , High glucose significantly decreased the mRNA levels of PI3K and Akt, which obviously increased by JDTL treatment in both INS-1 cells and HepG2 cells.

The protein expression of PI3K and Akt in INS-1 cells and HepG2 cells

In order to evaluate the consequences of network pharmacological analysis, we examined the effect of the JDTL on key proteins in the integrated “T2DM-related pathways” including PI3K/Akt signaling pathway using Western blot. We selected PI3K/Akt signaling pathway as the potential targets of T2DM combined with the basis of network pharmacology. Western blot analysis showed that high glucose group significantly decreased the expression of p-IRS, p-PI3K, p-AKT protein compared with the control group, while JDTL treatment inhibited this decrease in both INS-1 cells (Figure 14a,b) and HepG2 cells (Figure 14c,d).

### **Discussion**

T2DM is one of the most prominent and concerned chronic diseases due to its many complications, low cure rate and so on. For the treatment of T2DM, the treatment of TCM is also an indispensable part. TCM formula is an important part of component of TCM, is the most intuitive means to reflect the clinical curative effect, has been widely used in the clinical practice of TCM<sup>17</sup>. A variety of research reports suggest that the active ingredients in JDTL can regulate glucose levels. For example, the effective components of *Coptidis Rhizoma* can improve the disorder of glucose and lipid metabolism in T2DM through a variety of signaling pathways, and reduce the effect of glucose toxicity<sup>18,19</sup>. *Huangqi polysaccharides* have been used in the treatment and prevention of T2DM due to its ability to enhance immunity and improve insulin sensitivity<sup>20</sup>. *Salvia miltiorrhiza* Bunge can regulate colonic motility and intestinal neuron disturbance by reconstructing intestinal mechanical barrier in diabetic mice<sup>21</sup>. However, TCM formulas are often complicated in composition, so it is difficult to explain the mechanism of their intervention in disease. In the acreage of TCM research, arrangement pharmacology can use bioinformatics to adumbrate and analyze assorted biologic targets and interactions in disease so as to explain the atomic apparatus of TCM formulas from a added comprehensive perspective<sup>22,23</sup>.

The mechanism of JDTL in the treatment of T2DM was analyzed by network pharmacology, a total of 205 active components and 110 potential targets and 153 related signaling pathways were obtained in JDTL. The effective components of JDTL include quercetin, kaempferol, isorhamnetin, 7-O-methylisomucronulatol, beta-sitosterol and so on. Quercetin had the highest degree among the compounds, and it has many biological effects, such as anti-inflammatory, anti-tumor, anti-aging, antioxidant, vasodilator. It is a potential drug to improve T2DM and its cardiovascular complications<sup>24,25</sup>. Kaempferol can prevent obesity and insulin resistance induced by high-fat diet in mice, which may be realized by reducing insulin resistance<sup>26</sup>. It also can protect cardiomyocytes from hypoxia reoxygenation and endothelial cells from oxidative stress<sup>27</sup>. Some research reports point out that isorhamnetin could alleviate the injury induced by glucolipotoxicity in skeletal muscle cells, which may be related to the inhibition of JAK-STAT pathway activity<sup>28</sup>. These results indicate that JDTL has a synergistic effect in the treatment of T2DM, which reflects the characteristics of multi-component collaborative improvement of blood glucose.

Moreover, hub genes like AKT1, IL6, VEGFA, MAPK1, MAPK8, JUN, EGF, EGFR, CXCL8 and IL1B, and some signaling pathways such as PI3K-Akt signaling pathway, IL-17 signaling pathway, TNF signaling pathway, HIF-1 signaling pathway, and AGE-RAGE signaling pathway in diabetic complications, were filtered out as the basal mechanisms of JDTL in alleviative of T2DM. Therefore, SYBYL software was used for molecular docking of hub gene, which is closely related to the treatment of T2DM. Furthermore, the possible mechanism of JDTL inhibited T2DM development through regulating PI3K-Akt signaling pathway. Regarding the network pharmacology prediction results, we also use in vitro experiments to verify. The potential bioactive compounds, targets and signaling pathways of JDTL in the treatment of T2DM were identified for the first time.

The results of PPI network topology analysis showed that AKT1, IL6, VEGFA, MAPK1, MAPK8 were the top five important targets. And the results of molecular docking showed that quercetin and kaempferol have good interactions with VEGFA, MAPK1, and JUN. Isorhamnetin has good interactions with AKT1, IL6, and VEGFA.

Utilizing a literature-based investigation, we found that AKT1, IL6 and MAPK in core genes and PI3K/AKT pathways in concentrated pathways were closely related to glucometabolic. AKT is a serine/threonine protein kinase, a downstream signal protein of PI3K, which mediates cell proliferation, migration, differentiation, survival, or glucose metabolism<sup>29,30</sup>. Some experimental results showed that AKT1 was over expressed in the kidney of diabetic rats, and liraglutide could reduce the expression level of AKT1, hinder renal fibrosis and improve diabetic nephropathy<sup>31</sup>. In this study, IL6, another hub gene in the PPI network, is a pro-inflammatory cytokine, which also plays a complex role in the pathogenesis of T2DM. IL-6 is a cytokine with multiple functions, which can directly damage islet  $\beta$  cells and induce insulin resistance<sup>32</sup>. VEGFA is one of the members of VEGF family. It is a advance agency accompanying to angiogenesis and carefully accompanying to the accident and development of diabetic retinopathy<sup>33</sup>. It also can regulate angiogenesis and vascular permeability under physiological and pathological conditions, and VEGFA expression is closely related to diabetes<sup>34</sup>. MAPK1 and MAPK8 are members of mitogen-activated protein (MAP) kinase family. MAPK1, also known as extracellular regulated kinase (ERK), is mainly involved in cell proliferation and differentiation, oxidative stress and other physiological functions. Studies have shown that inhibition of MAPK1 protein expression can improve myocardial fibrosis in diabetic rats and reduce myocardial damage under high glucose condition<sup>35</sup>. Studies have shown that both insulin secretion and  $\beta$  cell mass dynamics are regulated by the related kinases of the AMPK family<sup>36</sup>. AMPK activation as an insulin sensitizer has attracted attention in the treatment of hyperglycemia in prediabetes, because it promotes the uptake of glucose in the muscles and shuts down the production of glucose in the liver during feeding, helping to restore normal blood sugar<sup>37</sup>.

In this study, we further explored the molecular mechanism of JDTL involved in insulin secretion and glucose uptake in INS-1 cells and HepG2 cells. PI3K-Akt signaling pathway, as a survival promoting signaling pathway, plays an important role in the process of islet cell proliferation, growth and apoptosis and lipid metabolism by mediating growth factor signal<sup>38,39</sup>. It is the main pathway of insulin signal

transduction and the main signal pathway of regulating blood glucose. The abnormality of PI3K/Akt signaling pathway is an important cause of diabetes<sup>40</sup>. The pathogenesis of T2DM is mainly related to insulin resistance<sup>41</sup>. Studies have found that the decreased expression of PI3K-Akt protein phosphorylation is the main mechanism leading to insulin resistance<sup>43</sup>. According to the results of cell experiment in vitro, The current study has further proven the therapeutic effect of JDTL on T2DM and examined and verified the results of the network pharmacology in advance(Figure 15).

### **Conclusions**

In conclusion, as JDTL is a TCM prescription formula, its components are complex and diverse, so we use the methods of network pharmacology and in vitro experimental verification to explore the active components, active components, targets, and pathways. We found 105 active ingredients that can directly affect T2DM targets, we also found top 10 potential targets and 153 related signaling pathways for the treatment of T2DM. And the results from cells experiment showed that JDTL can increase insulin secretion of INS-1 cells and improve glucose uptake in HepG2 cells , and PI3K/Akt signaling pathway serve as the key points and principal pathways for T2DM treatment. Therefore, JDTL has good hypoglycemic and insulin secretion promoting effects that have great potential to become a promising anti-diabetes candidate.

### **Abbreviations**

T2DM:Type 2 diabetes mellitus, JDTL: Jiedu Tongluo Tiaogan Formula, PPI: protein-protein interaction, GO: Enrichment of Gene Ontology, KEGG: Kyoto Encyclopedia of Genes and Genomes, TCM: Traditional Chinese medicine, MW: Molecular Weight, LogP: Octanol-Water Partition Coefficient, Hdon: The Number of Donor Atoms For H-Bonds, Hacc: The Number of Acceptor Atoms For H-Bonds, OB: Oral Bioavailability, DL: Drug-Like, TCMSP: Traditional Chinese Medicine Systems Pharmacology, MTT:3-(4,5-dimethylthiazol-2-yl)-2, 5-diphenyltetrazolium bromide, AKT1:RAC-alpha serine/threonine-protein kinase, IL-6:interleukin-6, VEGFA: vascular endothelial growth factor A, MAPK1:mitogen-activated protein kinase 1,

MAPK8:mitogen-activated protein kinase8,JUN: Transcription factor AP-1, EGF: Pro-epidermal growth factor, EGFR: Epidermal growth factor receptor, CXCL8: Interleukin-8, IL1B: Interleukin-1 beta, MF: molecular function, CC: cellular composition, BP: biological process.

### **Acknowledgments**

We appreciate the financial support received from the National Natural Science Foundation of China (grant number: 81973813) and Shenzhen Science and Technology Innovation Program (grant number: JCY20190809110015528).

### **Authors' contributions**

Qi Zhang and Chunli Piao contributed equally to this work. Fengmei Lian and Chunli Piao conceived and designed the research methods. Han Wang, Cheng Tang, Naiwen Zhang, Xiaohua Zhao and Shengnan Gao collected the data. Qi Zhang and Wenqi Jin analyzed the data. Qi Zhang, Wenqi Jin and De Jin carried out the experimental validation, and drafted the manuscript. All authors read and approved the final manuscript.

### **Funding**

This study was supported by the National Natural Science Foundation of China (grant number:81973813) and Shenzhen Science and Technology Innovation Program (grant number: JCY20190809110015528).

### **Availability of data and materials**

The raw data supporting the conclusions of this article will be made available by the authors, without undue reservation, to any qualified researcher.

### **Competing interests**

All authors declare no conflicts of interest.

### **Ethics approval and consent to participate**

Not applicable.

### **Consent for publication**

Not applicable.

## References

1. Inaishi Jun, Saisho Yoshifumi, Beta-Cell Mass in Obesity and Type 2 Diabetes, and Its Relation to Pancreas Fat: A Mini-Review. *Nutrients*, 2020, 12: undefined.
2. Aguilar-Ballester María, Hurtado-Genovés Gema, Taberner-Cortés Alida et al. Therapies for the Treatment of Cardiovascular Disease Associated with Type 2 Diabetes and Dyslipidemia. *Int J Mol Sci*, 2021, 22: undefined.
3. Mei Yu, Xiaoqing Zhan, Zhenxing Yang et al. Measuring the global, regional, and national burden of type 2 diabetes and the attributable risk factors in all 194 countries. *J Diabetes*, 2021, undefined: undefined.
4. Jung Chan Hee, Mok Ji Oh, Recent Updates on Vascular Complications in Patients with Type 2 Diabetes Mellitus. *Endocrinol Metab (Seoul)*, 2020, 35: 260-271.
5. Zheng Li, Chengyin Ye, Tianyu Zhao et al. Model of genetic and environmental factors associated with type 2 diabetes mellitus in a Chinese Han population. *BMC Public Health*, 2020, 20: 1024.
6. Kim Kibum, Unni Sudhir, McAdam Marx Carrie et al. Influence of Treatment Intensification on A1c in Patients with Suboptimally Controlled Type 2 Diabetes After 2 Oral Antidiabetic Agents. *J Manag Care Spec Pharm*, 2019, 25: 314-322.
7. Xin Wang, Ziyi Wang, Jiahui Zheng et al. TCM network pharmacology: A new trend towards combining computational, experimental and clinical approaches. *Chin J Nat Med*, 2021, 19: 1-11.
8. Zebiao Cao, Zhili Zeng, Baohua Wang et al. Identification of potential bioactive compounds and mechanisms of GegenQinlian decoction on improving insulin resistance in adipose, liver, and muscle tissue by integrating system pharmacology and bioinformatics analysis. *J Ethnopharmacol*, 2021, 264: 113289.
9. Meiyong Jin, Chunli Piao, Weiwei Pan, et al. Clinical observation on Jiedu Tongluo tiaogan decoction combined with abdominal acupuncture in the treatment of obese type 2 diabetes mellitus. *Cardiovascular Disease Electronic Journal of Integrated Traditional Chinese and Western Medicine*, 2020, 8(08):169-170.
10. Chunli Piao, Meiyong Jin, Zongjiang Zhao, et al. Effect of Jiedu Tongluo tiaogan Recipe on expression of IRE1 / JNK pathway related proteins in pancreas of ZDF rats with type 2 diabetes mellitus. *Chinese Archives of Traditional Chinese Medicine*, 2018, 36(01), 11-13.
11. Xiaotian Jiang, Chunli Piao, Jia Mi, et al. Effects of Jiedu Tongluo Tiaogan formula on the endoplasmic reticulum stress and inflammation of adipocytes. *Journal of Beijing University of Traditional Chinese Medicine*, 2018, 41(12), 1012-1018+1024.
12. Shasha He, Jingxia Zhao, Xiaolong Xu et al. Uncovering the Molecular Mechanism of the Qiang-Xin 1 Formula on Sepsis-Induced Cardiac Dysfunction Based on Systems Pharmacology. *Oxid Med Cell Longev*, 2020, 2020: 3815185.

13. Boezio B, Audouze K, Ducrot P, Taboureau O. Network-based Approaches in Pharmacology. *Mol Inform.* 2017 Oct;36(10).
14. Piao C, Zhang Q, Jin D, Wang L, Tang C, Zhang N, Lian F, Tong X. A Study on the Mechanism of Milkvetch Root in the Treatment of Diabetic Nephropathy Based on Network Pharmacology. *Evid Based Complement Alternat Med.* 2020 Oct 31;2020:6754761.
15. S. He, F. Liu, L. Xu et al., Protective effects of ferulic acid against heat stress-induced intestinal epithelial barrier dysfunction in vitro and in vivo. *PLoS One*, 2016 11:e145236.
16. Zeye Zhang, Jia Liu , Yifan Liu et al. Virtual screening of the multi-gene regulatory molecular mechanism of Si-Wu-tang against non-triple-negative breast cancer based on network pharmacology combined with experimental validation. *J Ethnopharmacol*, 2020, 269: 113696.
17. Wenjie Zheng, Gaofeng Wang, Zhe Zhang et al. Research progress on classical traditional Chinese medicine formula Liuwei Dihuang pills in the treatment of type 2 diabetes. *Biomed Pharmacother*, 2020, 121: 109564.
18. Zhong Y, Jin J, Liu P, et al. Berberine attenuates hyperglycemia by inhibiting the hepatic glucagon path way in diabetic mice. *Oxid Med Cell Longev*, 2020, 2020:6210526.
19. Cui L, Liu M, Chang X, et al. The inhibiting effect of the *Coptis chinensis* polysaccharide on the type type II diabetic mice. *Biomed Pharmacother*, 2016, 81: 111-119.
20. Cui K, Zhang SB, Jiang X, et al. Novel synergic antidiabetic effects of *Astragalus* polysaccharides combined with *Crataegus* flavonoids via improvement of islet function and liver metabolism. *Mol Med Rep*, 2016, 13(6):4737-4744.
21. Gu J F, Su S L, Guo J M, et al. The aerial parts of *Salvia miltiorrhiza* Bge. strengthen intestinal barrier and modulate gut microbiota imbalance in streptozocin-induced diabetic mice. *J Funct Foods* , 2017, 36:362-374.
22. Wang Z, Liu J, Yu Y, Chen Y, Wang Y. Modular pharmacology: the next paradigm in drug discovery. *Expert Opin Drug Discov.* 2012;7 (8):667–677. 3
23. Jing C, Sun Z, Xie X, et al. Network pharmacology-based identification of the key mechanism of Qinghuo Rougan Formula acting on uveitis. *Biomed Pharmacother.* 2019;120:109381.
24. Patel RV, Mistry BM, Shindesk, et al. Therapeutic potential of quercetin as a cardiovascular agent. *Eur J Med Chem*, 2018, 155:889-904
25. Roslan J , Giribabu N , Karim K , et al. Quercetin ameliorates oxidative stress, inflammation and apoptosis in the heart of streptozotocin-nicotinamide-induced adult male diabetic rats. *Biomedecine pharmacotherapie*, 2016, 86:570.
26. Tieqiao Wang, Qiaomin Wu, Tingqi Zhao, Preventive Effects of Kaempferol on High-Fat Diet-Induced Obesity Complications in C57BL/6 Mice. *Biomed Res Int*, 2020, 2020: 4532482.
27. Olazarán-Santibañez Fabián, Rivera Gildardo, Vanoye-Eligio Venancio et al. *Equisetum*

- Myriochoetum Antioxidant and Antiproliferative Activity of The Ethanol Extract of and Molecular Docking of Its Main Metabolites (Apigenin, Kaempferol, and Quercetin) on  $\beta$ -Tubulin. *Molecules*, 2021, 26: undefined.
28. Jiang H, Yamashita Y, Nakamura A, et al. Quercetin and its metabolite isorhamnetin promote glucose uptake through different signalling pathways in myotubes. *Sci Rep*, 2019, 9: 2690.
29. ALBURY-WARREN T M, PANDEY V, SPINEL L P, et al. Prediabetes linked to excess glucagon in transgenic mice with pancreatic active AKT1. *J Endocrinol*, 2016, 228(1): 49-59.
30. ALWHAIBI A, VERMA A, ADIL M S, et al. The unconventional role of Akt1 in the advanced cancers and in diabetes-promoted carcinogenesis. *Pharmacological Research*, 2019, 145: 104270.
31. Liao TT, Zhao LB, Liu H et al. Liraglutide protects from renal damage via Akt-mTOR pathway in rats with diabetic kidney disease. *Eur Rev Med Pharmacol Sci*, 2019, 23: 117-125.
32. Abad-Jiménez Zaida, López-Domènech Sandra, Díaz-Rúa Rubén et al. Systemic Oxidative Stress and Visceral Adipose Tissue Mediators of NLRP3 Inflammasome and Autophagy Are Reduced in Obese Type 2 Diabetic Patients Treated with Metformin. *Antioxidants (Basel)*, 2020, 9: undefined.
33. Liming Hu, Chunmei Gong, Xiaoping Chen et al. Associations between Vascular Endothelial Growth Factor Gene Polymorphisms and Different Types of Diabetic Retinopathy Susceptibility: A Systematic Review and Meta-Analysis. *J Diabetes Res*, 2021, 2021: 7059139.
34. Sellami N, Lamine LB, Turki A, et al. Association of VEGFA variants with altered VEGF secretion and type 2 diabetes: A case-control study. *Cytokine*, 2018, 106: 29.
35. Li Fang, Zeng Ou, Luo Jian et al. Effects of hydrogen sulfide on myocardial fibrosis and MAPK1/3 and MMP-8 expression in diabetic rats. *Nan Fang Yi Ke Da Xue Xue Bao*, 2015, 35: 549-52.
36. Rourke Jillian L, Hu Queenie, Sreaton Robert A, AMPK and Friends: Central Regulators of  $\beta$  Cell Biology. *Trends Endocrinol Metab*, 2018, 29: 111-122.
37. Coughlan, K.A. et al. (2014) AMPK activation: a therapeutic target for type 2 diabetes? *Diabetes Metab. Syndr. Obes.* 7, 241–253
38. Lee Jinjoo, Noh Seungjin, Lim Suhyun et al. Plant Extracts for Type 2 Diabetes: From Traditional Medicine to Modern Drug Discovery. *Antioxidants (Basel)*, 2021, 10: undefined.
39. Guo Sa, Ouyang Hui, Du Wendi et al. Gynura procumbens Exploring the protective effect of against type 2 diabetes mellitus by network pharmacology and validation in C57BL/KsJ db/db mice. *Food Funct*, 2021, undefined: undefined.
40. Huang XJ, Liu GH, Guo J, et al. The PI3K/Akt pathway in obesity and type 2 diabetes. *Int J Biol Sci*, 2018, 14: 1483-1496.

41. Boughanem Hatim, Yubero-Serrano Elena M, López-Miranda José et al. Potential Role of Insulin Growth-Factor-Binding Protein 2 as Therapeutic Target for Obesity-Related Insulin Resistance. *Int J Mol Sci*, 2021, 22: undefined.

42. Breen Danna M, Giacca Adria, Effects of insulin on the vasculature. *Curr Vasc Pharmacol*, 2011, 9: 321-32.

## Figure legends

**Figure 1** Workflow for the mechanism of JDTL in treating T2DM.

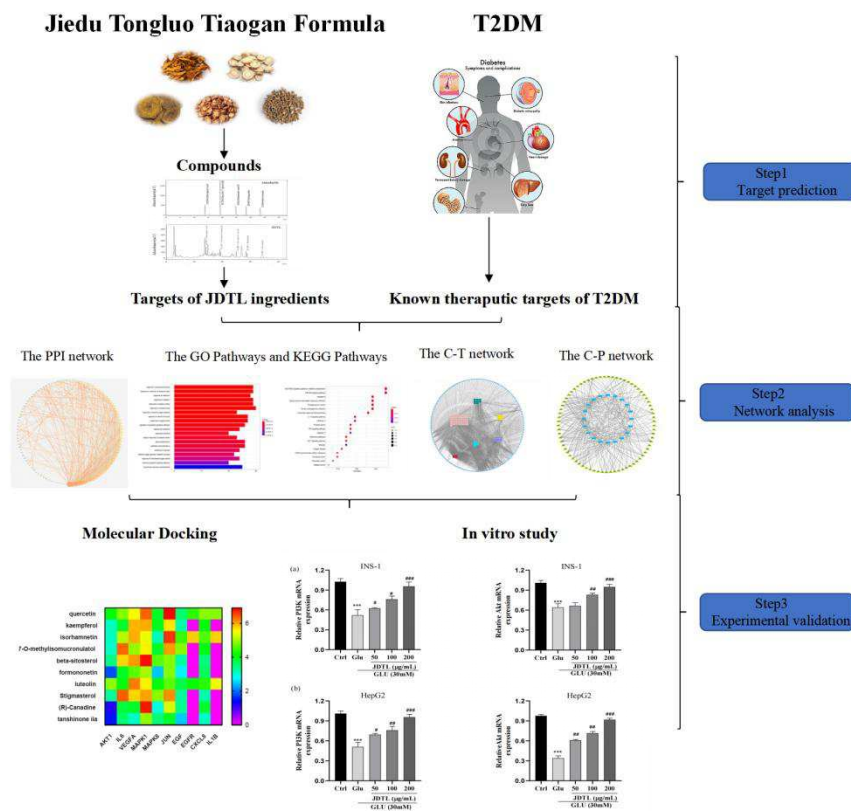


**Figure 2** JDTL levels were determined using HPLC.

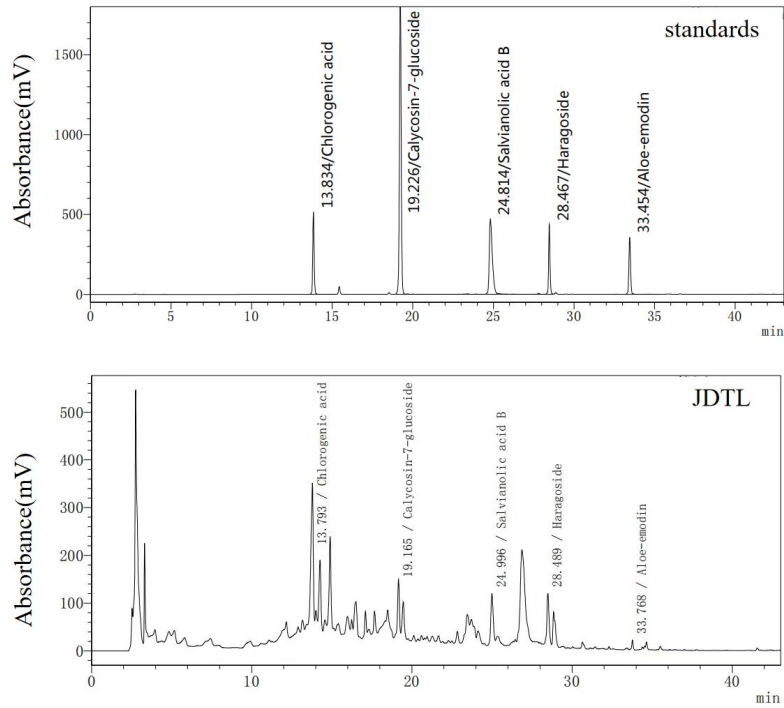


**Figure 3** The venn diagram of the common targets.

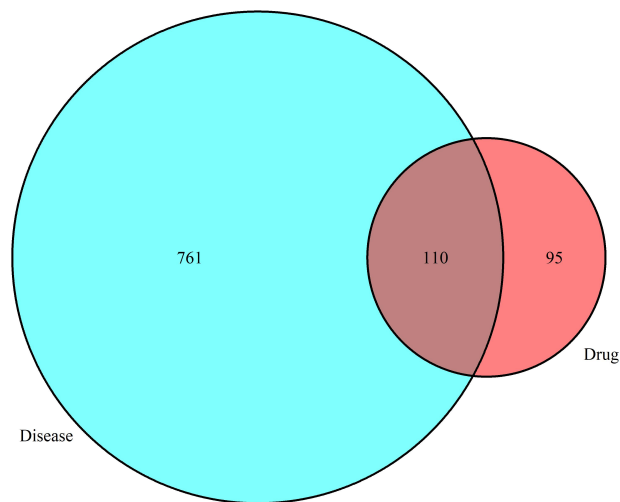
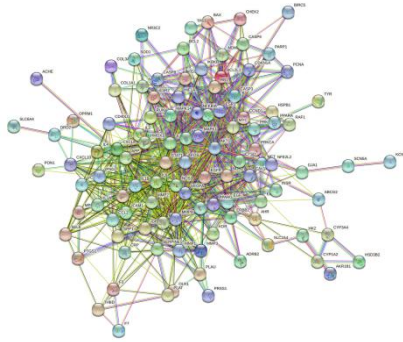
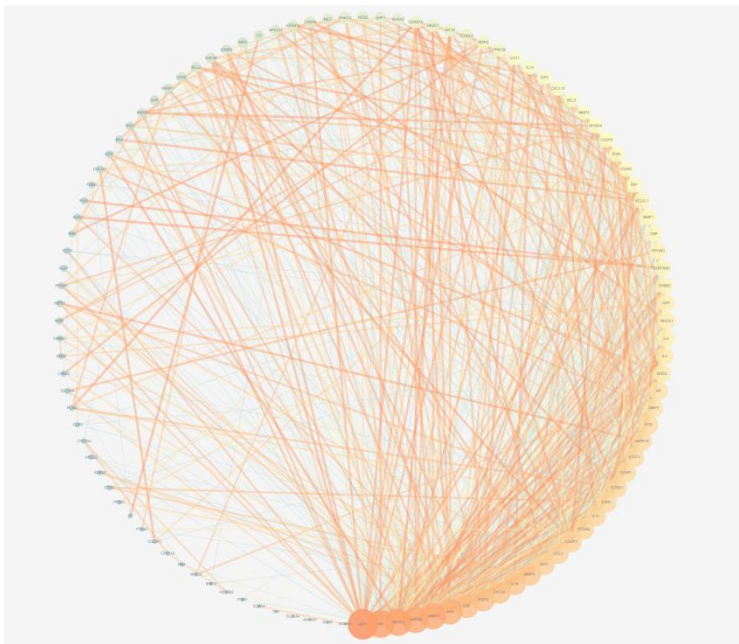


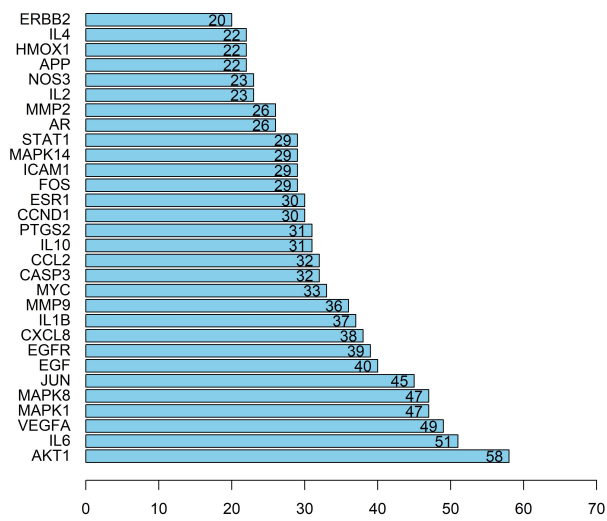
**Figure 4(a,b,c)** PPI network of compound-T2DM-related protein. (a) The PPI network by built in the String Database;(b)The PPI network by established in the Cytoscape 3.7.2; (c)The bar plot of the PPI network.



(a) The PPI network by built in the String Database;



(b) The PPI network by established in the Cytoscape 3.7.2;



(c)The bar plot of the PPI network.

**Figure 5(a,b,c)** GO analysis for the major targets of JDTL. (a) Bar chart of molecular function categories; (b) Bar chart of cellular composition categories; (c) Bar chart of biological process categories. ( $P < 0.05$ )

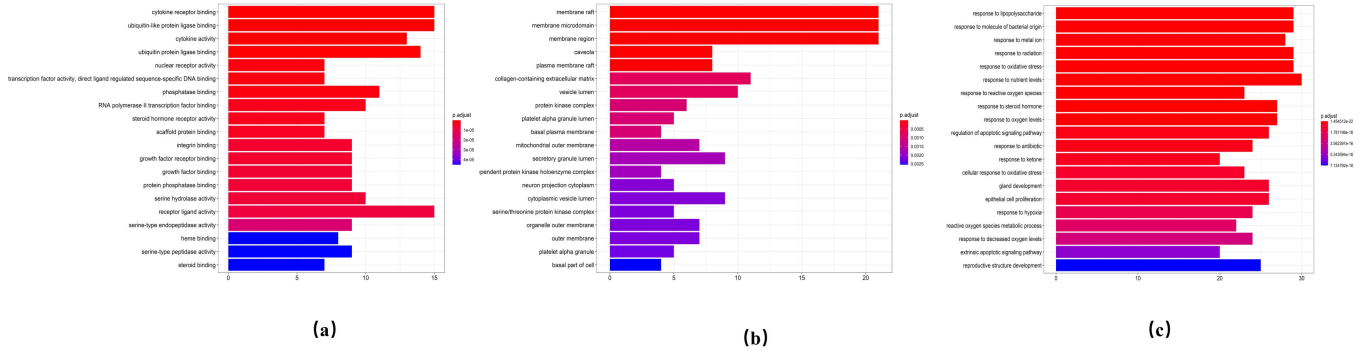
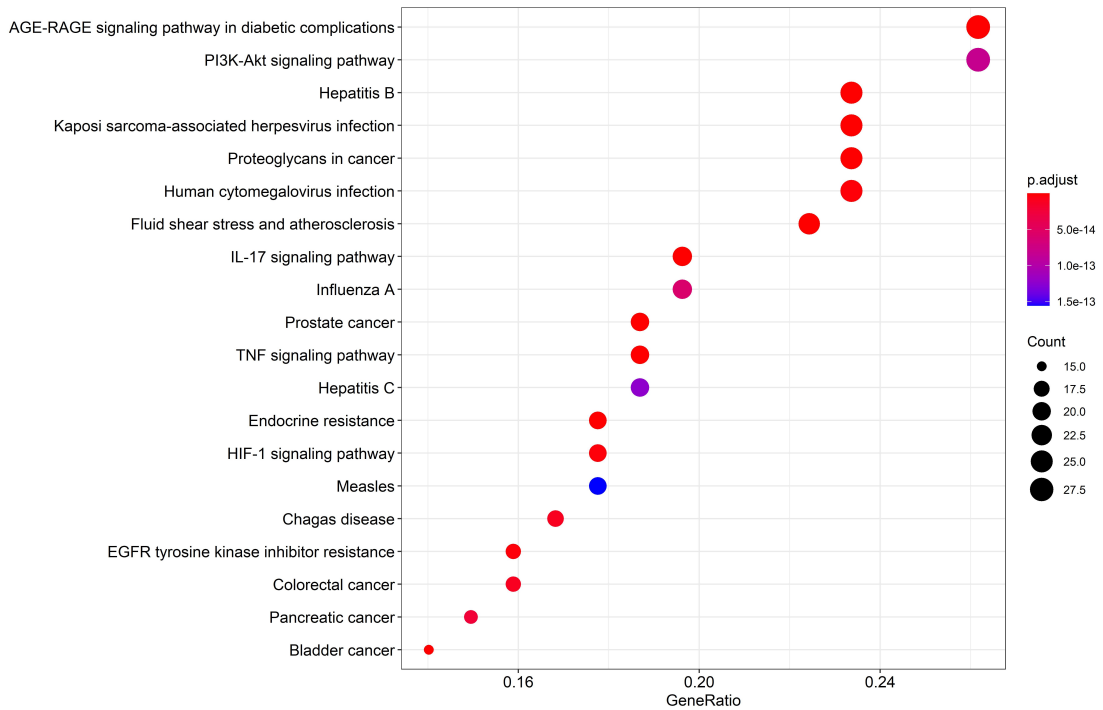
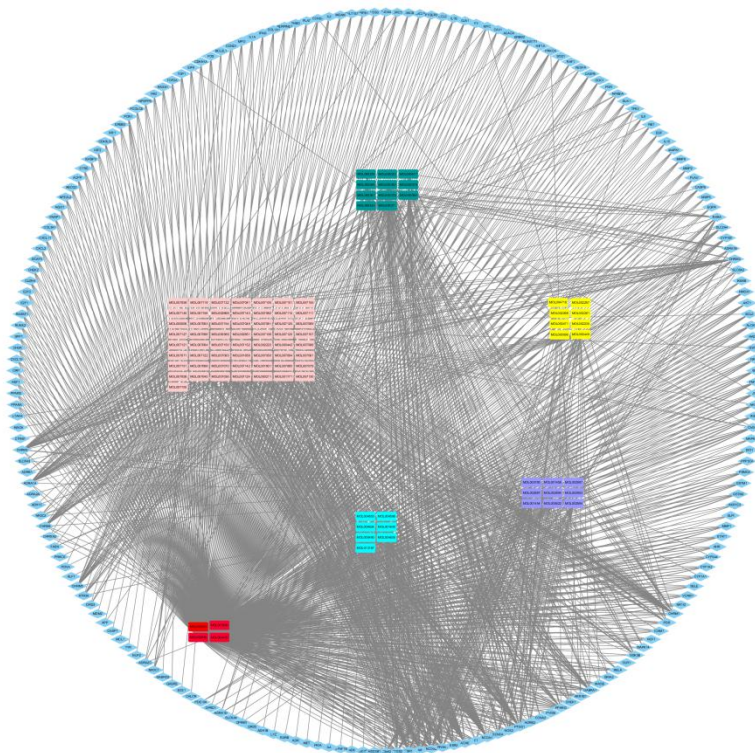


**Figure 6** KEGG analysis for the major targets of JDTL. The x-axis and the y-axis represent the counts of the target symbols in each pathway and the main pathway, respectively. ( $P < 0.05$ )



**Figures 7** Compound-compound target network of JDTL. Yellow rectangle, light blue rectangle, purple rectangle, dark green rectangle and pink rectangle

represent Dahuang, Chaihu, Huanglian, Huangqi and Danshen respectively. Red rectangle represent repetitive compounds, and blue rhombus denote compound target.



**Figures 8** The top 20 Pathway of JDTL-T2DM network. 73 T2DM related target nodes represented by green Triangle, and 20 pathway nodes described by blue rectangle.

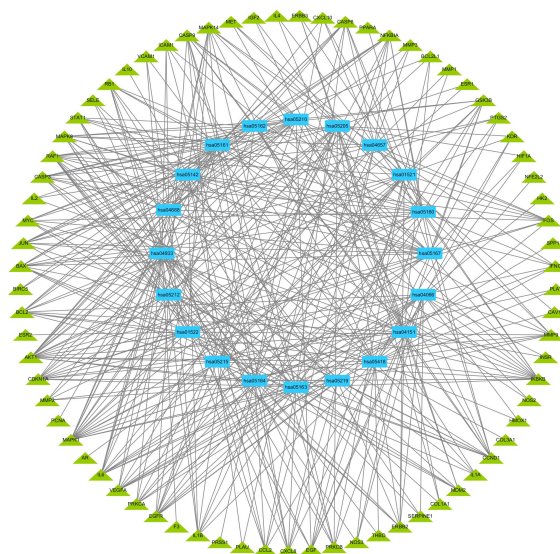


**Figure 9** The molecular docking result of compound and hub gene.

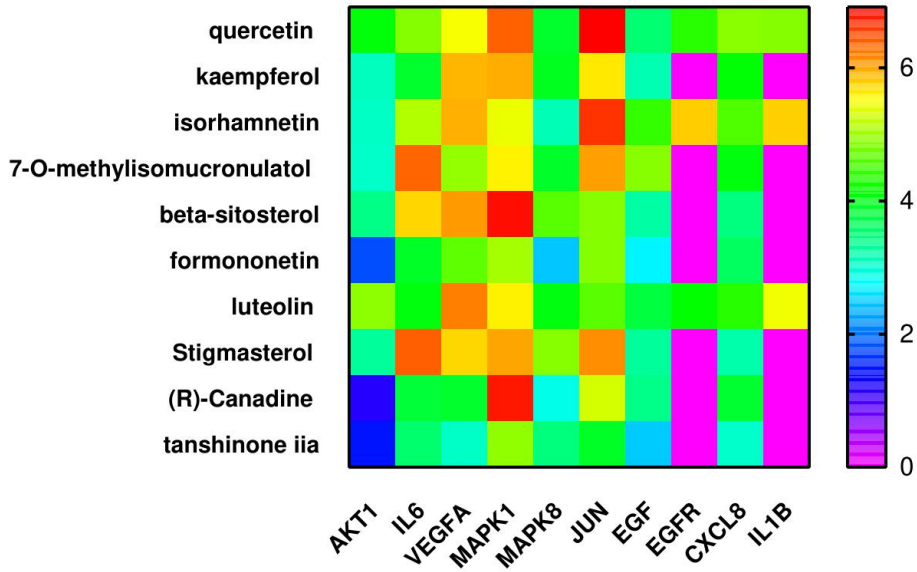


**Figure 10** Effects of JDTL on cell viability. INS-1 cells and HepG2 cells were respectively treated with different concentrations of JDTL for 24 hours, and cell viabilities were detected by MTT method. Values are means  $\pm$  SD from three independent experiments,  $^{\#}P < 0.05$  compared to Control.

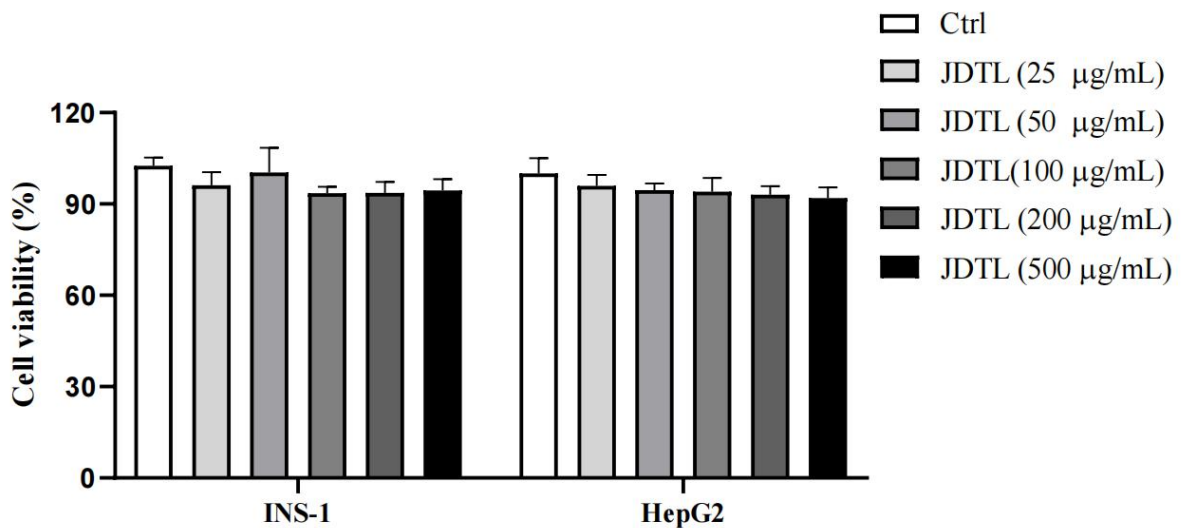


**Figure 11** Effect of JDTL on INS-1 cell insulin secretion. Values are means  $\pm$  SD from three independent experiments.

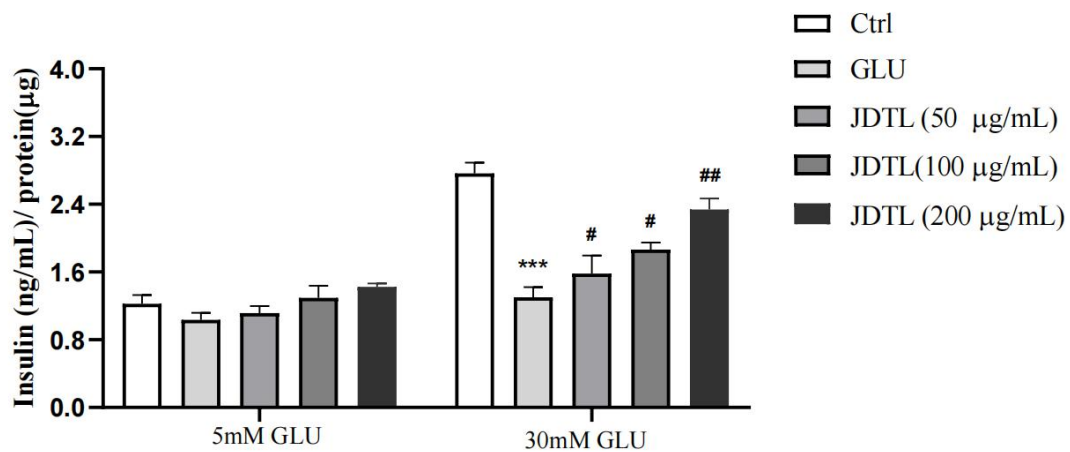


**Figure 12** Effects of JDTL on glucose uptake in HepG2 cells. The fluorescence intensity of 2-NBDG into HepG2 cells. Values are means  $\pm$  SD from three independent experiments.

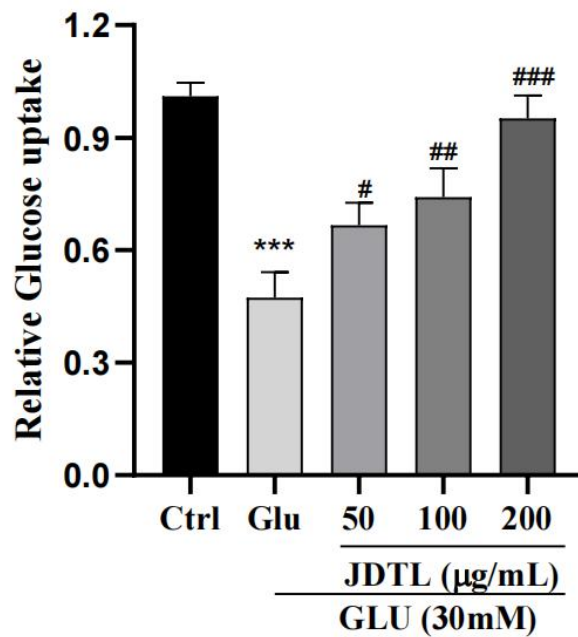


**Figure 13(a,b)** Effects of JDTL on the expression levels of PI3K and Akt. (a) in INS-1 cells. (b) in HepG2 cells. Values are means  $\pm$  SD from three independent experiments. \*\*\* $P$ <0.01. # $P$ <0.05, ## $P$ <0.01, ### $P$ <0.001 compared to the model.

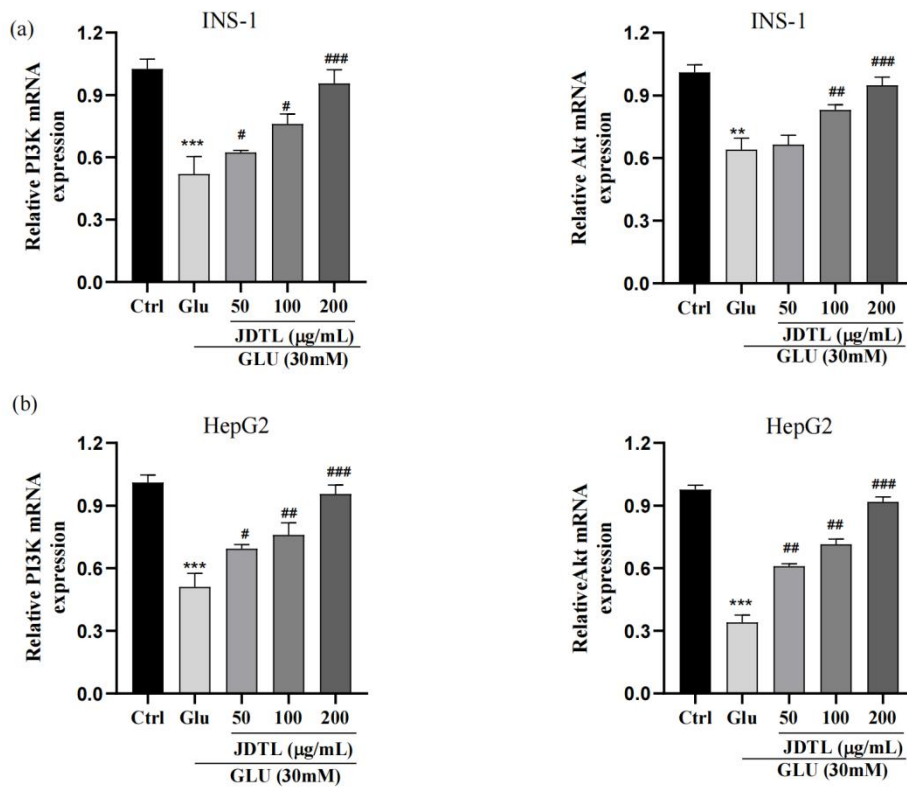
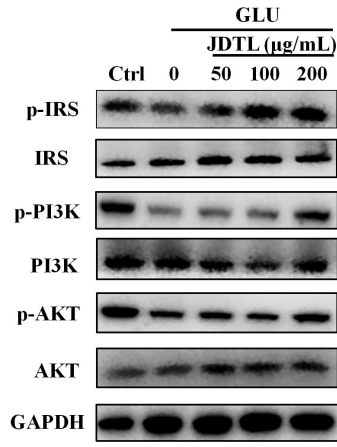
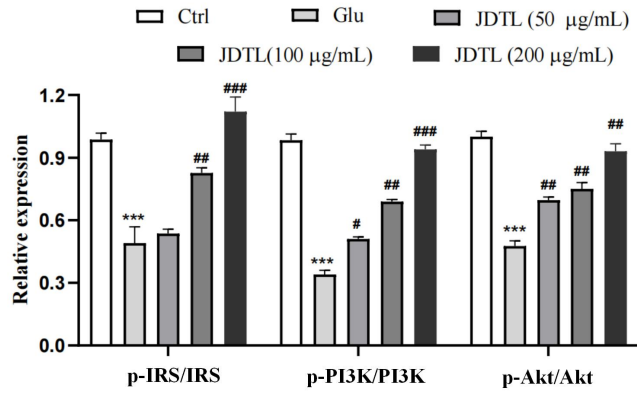


**Figure 14(a,b,c,d)** Effects of JDTL on the IRS-1/PI3K/Akt protein expression. (a) in INS-1 cells. (c) in HepG2 cells. Cell lysates were subjected to Western blot analysis using GAPDH as a loading control. (b,d) Quantification of bands relative to GAPDH using Image J software. Values are means  $\pm$  SD from three independent experiments. \*\*\* $P$ <0.001. # $P$ <0.05, ## $P$ <0.01, ### $P$ <0.001 compared to the model.

## INS-1

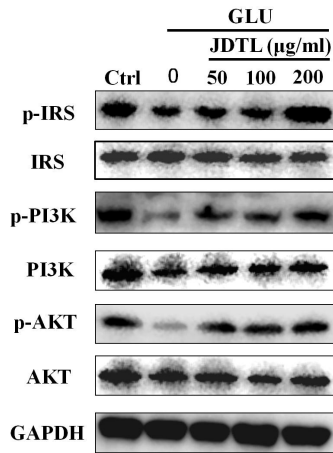


(a)

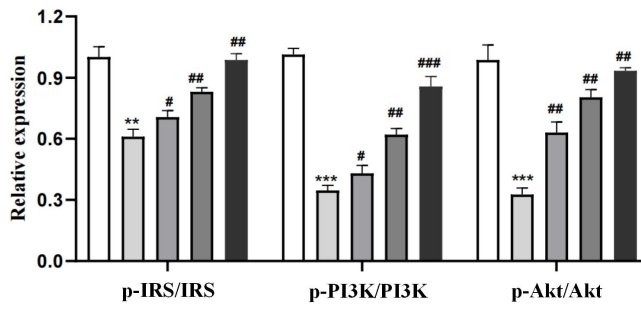


(b)

## HepG2



(c)



(d)

**Figure 15** Potential metabolic pathways regulated in T2DM after treatment with JDTL Formula.

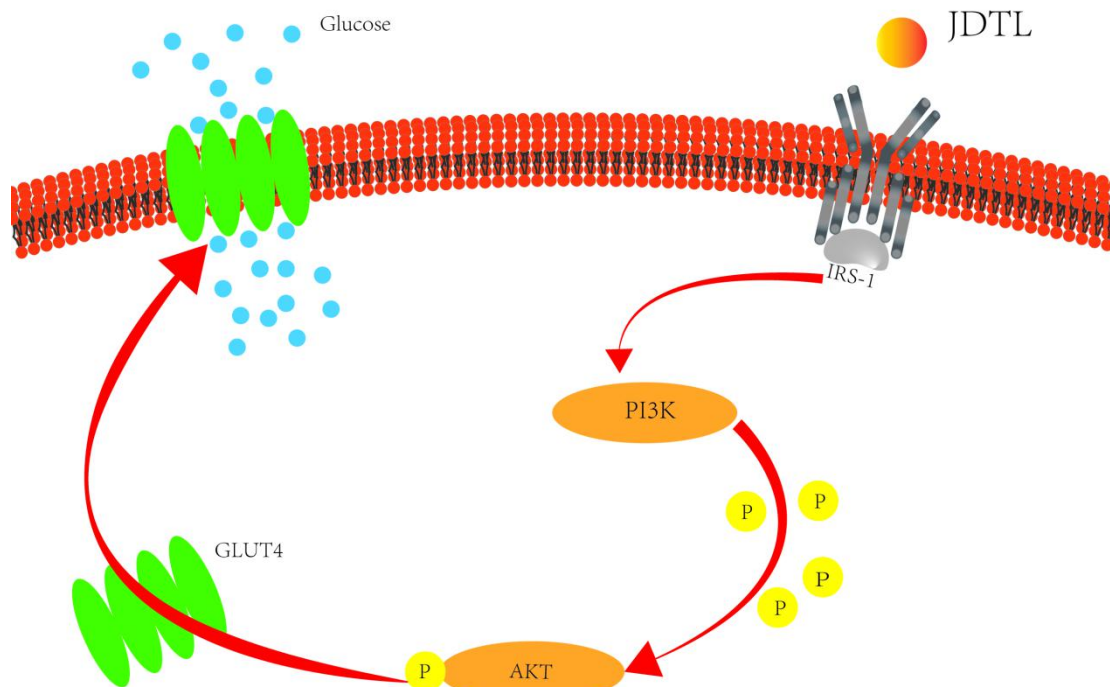


**Table 1** Potential Active Ingredients of JDTL

Mol ID	Compound	OB	DL	Medicine
MOL002235	EUPATIN	50.8	0.41	Dahuang
MOL002268	rhein	47.07	0.28	Dahuang
MOL002281	Toralactone	46.46	0.24	Dahuang
MOL002297	Daucosterol_qt	35.89	0.7	Dahuang
MOL000471	aloe-emodin	83.38	0.24	Dahuang
MOL000096	(-)-catechin	49.68	0.24	Dahuang
MOL002251	Mutatochrome	48.64	0.61	Dahuang
MOL002259	Physciondiglucoside	41.65	0.63	Dahuang
MOL002260	Procyanidin B-5,3'-O-gallate	31.99	0.32	Dahuang
MOL002276	Sennoside E_qt	50.69	0.61	Dahuang

MOL002280	Torachryson-8-O-beta-D-(6'-oxayl)-glucoside	43.02	0.74	Dahuang
MOL002288	Emodin-1-O-beta-D-glucopyranoside	44.81	0.8	Dahuang
MOL002293	Sennoside D Qt	61.06	0.61	Dahuang
MOL002303	palmidin A	32.45	0.65	Dahuang
MOL000358	beta-sitosterol	36.91	0.75	Dahuang
MOL000554	Gallic acid-3-O-(6'-O-galloyl)-glucoside	30.25	0.67	Dahuang
MOL004718	$\alpha$ -spinasterol	42.98	0.76	Chaihu
MOL000449	Stigmasterol	43.83	0.76	Chaihu
MOL004653	(+)-Anomalin	46.06	0.66	Chaihu
MOL004598	3,5,6,7-tetramethoxy-2-(3,4,5-trimethoxyphenyl)chromone	31.97	0.59	Chaihu
MOL004609	Areapillin	48.96	0.41	Chaihu
MOL001645	Linoleyl acetate	42.1	0.2	Chaihu
MOL004624	Longikaurin A	47.72	0.53	Chaihu
MOL004609	Areapillin	48.96	0.41	Chaihu
MOL013187	Cubebin	57.13	0.64	Chaihu
MOL000354	isorhamnetin	49.6	0.31	Chaihu
MOL004628	Octalupine	47.82	0.28	Chaihu
MOL004644	Sainfuran	79.91	0.23	Chaihu
MOL001454	berberine	36.86	0.78	Huanglian
MOL013352	Obacunone	43.29	0.77	Huanglian
MOL002894	berberrubine	35.74	0.73	Huanglian
MOL002897	epiberberine	43.09	0.78	Huanglian
MOL002903	(R)-Canadine	55.37	0.77	Huanglian
MOL002904	Berlambine	36.68	0.82	Huanglian
MOL002907	Corchoroside A Qt	104.95	0.78	Huanglian
MOL000622	Magnograndiolide	63.71	0.19	Huanglian
MOL000762	Palmidin A	35.36	0.65	Huanglian

MOL000785	palmatine	64.6	0.65	Huanglian
MOL001458	coptisine	30.67	0.86	Huanglian
MOL002668	Worenine	45.83	0.87	Huanglian
MOL008647	Moupinamide	86.71	0.26	Huanglian
MOL000211	Mairin	55.38	0.78	Huangqi
MOL000239	Jaranol	50.83	0.29	Huangqi
MOL000296	hederagenin	36.91	0.75	Huangqi
MOL000033	(3S,8S,9S,10R,13R,14S,17R)-10,13-dimethyl-17-[(2R,5S)-5-propan-2-yl]octan-2-yl]-2,3,4,7,8,9,11,12,14,15,16,17-dodecahydro-1H-cyclopenta[a]phenanthren-3-ol	36.23	0.78	Huangqi
MOL000371	3,9-di-O-methylnissolin	53.74	0.48	Huangqi
MOL000374	5'-hydroxyiso-muronulatol-2',5'-di-O-glucoside	41.72	0.69	Huangqi
MOL000378	7-O-methylisomucronulatol	74.69	0.3	Huangqi
MOL000379	9,10-dimethoxypterocarpan-3-O-β-D-glucoside	36.74	0.92	Huangqi
MOL000380	(6aR,11aR)-9,10-dimethoxy-6a,11a-dihydro-6H-benzofurano[3,2-c]chromen-3-ol	64.26	0.42	Huangqi
MOL000387	Bifendate	31.1	0.67	Huangqi
MOL000392	formononetin	69.67	0.21	Huangqi
MOL000398	isoflavanone	109.99	0.3	Huangqi
MOL000417	Calycosin	47.75	0.24	Huangqi
MOL000433	FA	68.96	0.71	Huangqi
MOL000438	(3R)-3-(2-hydroxy-3,4-dimethoxyphenyl)chroman-7-ol	67.67	0.26	Huangqi
MOL000439	isomucronulatol-7,2'-di-O-glucoside	49.28	0.62	Huangqi
MOL001601	1,2,5,6-tetrahydrotanshinone	38.75	0.36	Danshen
MOL001659	Poriferasterol	43.83	0.76	Danshen

MOL001771	poriferast-5-en-3beta-ol	36.91	0.75	Danshen
MOL001942	isoimperatorin	45.46	0.23	Danshen
MOL002222	sugiol	36.11	0.28	Danshen
MOL002651	Dehydrotanshinone II A	43.76	0.4	Danshen
MOL002776	Baicalin	40.12	0.75	Danshen,Chai hu
MOL000569	digallate	61.85	0.26	Danshen
MOL000006	luteolin	36.16	0.25	Danshen
MOL006824	$\alpha$ -amyrin	39.51	0.76	Danshen
MOL007036	5,6-dihydroxy-7-isopropyl-1,1-dimethyl-2,3-dihydrophenanthren-4-one	33.77	0.29	Danshen
MOL007041	2-isopropyl-8-methylphenanthrene-3,4-dione	40.86	0.23	Danshen
MOL007045	3 $\alpha$ -hydroxytanshinone II a	44.93	0.44	Danshen
MOL007048	(E)-3-[2-(3,4-dihydroxyphenyl)-7-hydroxy-benzofuran-4-yl]acrylic acid	48.24	0.31	Danshen
MOL007049	4-methylenemiltirone	34.35	0.23	Danshen
MOL007050	2-(4-hydroxy-3-methoxyphenyl)-5-(3-hydroxypropyl)-7-methoxy-3-benzofurancarboxaldehyde	62.78	0.4	Danshen
MOL007051	6-o-syringyl-8-o-acetyl shanzhiside methyl ester	46.69	0.71	Danshen
MOL007058	formyltanshinone	73.44	0.42	Danshen
MOL007059	3-beta-Hydroxymethylenetanshinquinone	32.16	0.41	Danshen
MOL007061	Methylenetanshinquinone	37.07	0.36	Danshen
MOL007063	przewalskin a	37.11	0.65	Danshen
MOL007064	przewalskin b	110.32	0.44	Danshen
MOL007068	Przewaquinone B	62.24	0.41	Danshen
MOL007069	przewaquinone c	55.74	0.4	Danshen
MOL007070	(6S,7R)-6,7-dihydroxy-1,6-dimethyl-8,9-dih	41.31	0.45	Danshen

	ydro-7H-naphtho[8,7-g]benzofuran-10,11-dione			
MOL007071	przewaquinone f	40.31	0.46	Danshen
MOL007077	sclareol	43.67	0.21	Danshen
MOL007079	tanshinaldehyde	52.47	0.45	Danshen
MOL007081	Danshenol B	57.95	0.56	Danshen
MOL007082	Danshenol A	56.97	0.52	Danshen
MOL007085	Salvilenone	30.38	0.38	Danshen
MOL007088	cryptotanshinone	52.34	0.4	Danshen
MOL007093	dan-shexinkum d	38.88	0.55	Danshen
MOL007094	danshenspiroketallactone	50.43	0.31	Danshen
MOL007098	deoxyneocryptotanshinone	49.4	0.29	Danshen
MOL007100	dihydrotanshinlactone	38.68	0.32	Danshen
MOL007101	dihydrotanshinone I	45.04	0.36	Danshen
MOL007105	epidanshenspiroketallactone	68.27	0.31	Danshen
MOL007107	C09092	36.07	0.25	Danshen
MOL007108	isocryptotanshi-none	54.98	0.39	Danshen
MOL007111	Isotanshinone II	49.92	0.4	Danshen
MOL007115	manool	45.04	0.2	Danshen
MOL007118	microstegiol	39.61	0.28	Danshen
MOL007119	miltionone I	49.68	0.32	Danshen
MOL007120	miltionone II	71.03	0.44	Danshen
MOL007121	miltipolone	36.56	0.37	Danshen
MOL007122	Miltirone	38.76	0.25	Danshen
MOL007123	miltirone II	44.95	0.24	Danshen
MOL007124	neocryptotanshinone ii	39.46	0.23	Danshen
MOL007125	neocryptotanshinone	52.49	0.32	Danshen
MOL007127	1-methyl-8,9-dihydro-7H-naphtho[5,6-g]benzofuran-6,10,11-trione	34.72	0.37	Danshen

MOL007130	prolithospermic acid	64.37	0.31	Danshen
MOL007132	(2R)-3-(3,4-dihydroxyphenyl)-2-[(Z)-3-(3,4-dihydroxyphenyl)acryloyl]oxy-propionic acid	109.38	0.35	Danshen
MOL007140	(Z)-3-[2-[(E)-2-(3,4-dihydroxyphenyl)vinyl]-3,4-dihydroxy-phenyl]acrylic acid	88.54	0.26	Danshen
MOL007141	salvianolic acid g	45.56	0.61	Danshen
MOL007142	salvianolic acid j	43.38	0.72	Danshen
MOL007143	salvilenone l	32.43	0.23	Danshen
MOL007145	salviolone	31.72	0.24	Danshen
MOL007149	NSC 122421	34.49	0.28	Danshen
MOL007150	(6S)-6-hydroxy-1-methyl-6-methylol-8,9-dihydro-7H-naphtho[8,7-g]benzofuran-10,11-quinone	75.39	0.46	Danshen
MOL007151	Tanshindiol B	42.67	0.45	Danshen
MOL007152	Przewaquinone E	42.85	0.45	Danshen
MOL007154	tanshinone iia	49.89	0.4	Danshen
MOL007155	(6S)-6-(hydroxymethyl)-1,6-dimethyl-8,9-dihydro-7H-naphtho[8,7-g]benzofuran-10,11-dione	65.26	0.45	Danshen
MOL007156	tanshinone VI	45.64	0.3	Danshen
MOL000354	isorhamnetin	49.6	0.31	Chaihu,Huangqi
MOL000422	kaempferol	41.88	0.24	Chaihu,Huangqi,
MOL000098	quercetin	46.43	0.28	Chaihu,Huanglian,Huangqi
MOL000358	beta-sitosterol	36.91	0.75	Dahuang

**Table 2** KEGG pathways regulated by JDTL against T2DM

No.	Pathway ID	Pathway Name	P value	Count	Gene Name
1	hsa04933	AGE-RAGE signaling pathway in diabetic complications	1.41E-30	28	MAPK14/ICAM1/VCAM1/SELE/STAT1/MAPK8/CASP3/JUN/BAX/BCL2/AKT1/MMP2/MAPK1/IL6/VEGFA/PRKCA/F3/IL1B/CCL2/CXCL8/PRKCB/NOS3/THBD/SERPINE1/COL1A1/IL1A/CCND1/COL3A1
2	hsa05418	Fluid shear stress and atherosclerosis	8.98E-21	24	MAPK14/ICAM1/VCAM1/SELE/MAPK8/JUN/BCL2/AKT1/HMOX1/IKKBK/MMP2/MMP9/VEGFA/CAV1/IL1B/CCL2/NOS3/PLAT/THBD/IFNG/IL1A/FOS/NFE2L2/KDR
3	hsa04657	IL-17 signaling pathway	1.03E-20	21	PTGS2/GSK3B/MAPK14/MMP1/MAPK8/CASP3/JUN/IKKBK/MMP3/MMP9/MAPK1/IL6/NFKBIA/CASP8/IL1B/CCL2/CXCL8/IFNG/FOS/CXCL10/IL4
4	hsa05161	Hepatitis B	2.24E-20	25	MAPK14/STAT1/MAPK8/CASP3/JUN/BAX/BCL2/AKT1/IKKBK/CASP9/MMP9/MAPK1/RB1/IL6/NFKBIA/CASP8/RAF1/PRKCA/MYC/CXCL8/PRKCB/BIRC5/FOS/CDKN1A/PCNA
5	hsa05215	Prostate cancer	5.18E-19	20	AR/GSK3B/BCL2/AKT1/IKKBK/EGFR/MMP3/CASP9/PLAU/MMP9/MAPK1/EGF/RB1/NFKBIA/RAF1/ERBB2/PLAT/CCND1/CDKN1A/MDM2
6	hsa05219	Bladder cancer	1.17E-18	15	MMP1/EGFR/MMP2/MMP9/MAPK1/EGF/RB1/VEGFA/RAF1/ERBB2/MYC/CXCL8/CCND1/CDKN1A/MDM2
7	hsa05167	Kaposi sarcoma-associated herpesvirus infection	1.82E-18	25	PTGS2/GSK3B/MAPK14/ICAM1/STAT1/MAPK8/CASP3/JUN/BAX/AKT1/IKKBK/CASP9/MAPK1/RB1/IL6/NFKBIA/CASP8/VEGFA/RAF1/HIF1A/MYC/CXCL8/CCND1/FOS/CDKN1A
8	hsa05205	Proteoglycans in cancer	8.05E-18	25	ESR1/MAPK14/CASP3/AKT1/EGFR/PLAU/MMP2/MMP9/MAPK1/VEGFA/RAF1/PRKCA/HIF1A/ERBB2/CAV1/MYC/PRKCB/COL1A1/CCND1/CDKN1A/ERBB3/IGF2/MDM2/KDR/MET
9	hsa04668	TNF signaling pathway	1.06E-17	20	PTGS2/MAPK14/ICAM1/VCAM1/SELE/MAPK8/CASP3/JUN/AKT1/IKKBK/MMP3/MMP9/MAPK1/IL6/NFKBIA/CASP8/IL1B/CCL2/FOS/CXCL10
10	hsa01522	Endocrine resistance	1.47E-17	19	ESR1/ESR2/MAPK14/MAPK8/JUN/BAX/BCL2/AKT1/EGFR/MMP2/MMP9/MAPK1/RB1/RAF1/ERBB2/CCND1/FOS/CDKN1A/MDM2
11	hsa05163	Human cytomegalovirus infection	7.77E-17	25	PTGS2/GSK3B/MAPK14/CASP3/BAX/AKT1/IKKBK/EGFR/CASP9/MAPK1/RB1/IL6/NFKBIA/CASP8/VEGFA/RAF1/PRKCA/MYC/IL1B/CCL2/CXCL8/PRKCB/CCND1/CDKN1A/MDM2
12	hsa04066	HIF-1 signaling pathway	1.21E-16	19	NOS2/INSR/BCL2/AKT1/HMOX1/EGFR/MAPK1/EGF/IL6/VEGFA/PRKCA/HIF1A/ERBB2/PRKCB/NOS3/SERPINE1/IFNG/CDKN1A/HK2
13	hsa01521	EGFR tyrosine kinase inhibitor resistance	1.30E-16	17	GSK3B/BAX/BCL2/AKT1/EGFR/MAPK1/EGF/IL6/VEGFA/RAF1/PRKCA/ERBB2/PRKCB/BCL2L1/ERBB3/KDR/MET
14	hsa05210	Colorectal cancer	6.01E-16	17	GSK3B/MAPK8/CASP3/JUN/BAX/BCL2/AKT1/EGFR/CASP9/MAPK1/EGF/RAF1/MYC/BIRC5/CCND1/FOS/CDKN1A
15	hsa05142	Chagas disease	6.55E-16	18	NOS2/MAPK14/MAPK8/JUN/AKT1/IKKBK/MAPK1/IL10/IL6/NFKBIA/CASP8/IL1B/CCL2/CXCL8/IL2/SERPINE1/IFNG/FOS
16	hsa05212	Pancreatic cancer	1.59E-15	16	STAT1/MAPK8/BAX/AKT1/IKKBK/EGFR/CASP9/MAPK1/EGF/RB1/VEGFA/RAF1/ERBB2/CCND1/BCL2L1/CDKN1A
17	hsa05164	Influenza A	4.13E-15	21	PRSS1/ICAM1/STAT1/CASP3/BAX/AKT1/IKKBK/CASP9/MAPK1/IL6/NFKBIA/CASP8/RAF1/PRKCA/IL1B/CCL2/CXCL8/PRKCB/IFNG/IL1A/CXCL10
18	hsa04151	PI3K-Akt signaling pathway	6.14E-15	28	GSK3B/INSR/BCL2/AKT1/IKKBK/EGFR/CASP9/MAPK1/EGF/IL6/VEGFA/RAF1/PRKCA/ERBB2/MYC/NOS3/IL2/COL1A1/CCND1/BCL2L1/CDKN1A/ERBB3/IGF2/SPPI/MDM2/KDR/MET/IL4
19	hsa05160	Hepatitis C	9.78E-15	20	GSK3B/STAT1/CASP3/BAX/AKT1/IKKBK/EGFR/CASP9/MAPK1/EGF/RB1/NFKBIA/CASP8/RAF1/MYC/IFNG/CCND1/CDKN1A/CXCL10/PPARA
20	hsa05162	Measles	1.30E-14	19	GSK3B/STAT1/MAPK8/CASP3/JUN/BAX/BCL2/AKT1/IKKBK/CASP9/IL6/NFKBIA/CASP8/IL1B/IL2/IL1A/CCND1/BCL2L1/FOS

**Table 3** The docking information of 10 targets with the corresponding compounds.

bioactive components	docking scores									
	AKT1	IL6	VEGFA	MAPK1	MAPK8	JUN	EGF	EGFR	CXCL8	IL1B
quercetin	4.8722	5.491	6.3808	3.9012	6.9138	3.5311	4.3696	4.895	4.8696	4.8722
kaempferol	3.9056	5.9222	5.9673	3.978	5.6494	3.1839	0	4.1176	0	3.9056
isorhamnetin	5.1164	5.9582	5.4267	3.1612	6.6275	4.4309	5.7929	4.5729	5.7761	5.1164
7-O-methylisomucronulatol	6.3561	4.9481	5.5891	3.9192	6.0454	4.8871	0	4.0729	0	6.3561
beta-sitosterol	5.7526	6.0651	6.8363	4.6171	4.8629	3.2453	0	3.4631	0	5.7526
formononetin	3.9304	4.6556	5.0389	2.4642	4.8664	2.7135	0	3.6248	0	3.9304
luteolin	4.0717	6.2124	5.5947	4.0627	4.6269	3.8032	4.164	4.3608	5.4624	4.0717
Stigmasterol	6.3914	5.7478	6.0177	4.8827	6.1335	3.3023	0	3.2264	0	6.3914
(R)-Canadine	3.8318	3.8965	6.7875	2.8945	5.3026	3.4048	0	3.8857	0	3.8318
tanshinone iia	3.549	3.0598	4.9401	3.4755	3.9263	2.4784	0	3.05	0	3.549